ELSEVIER

Biochimica et Biophysica Acta 1561 (2002) 251–265

BIOCHIMICA ET BIOPHYSICA ACTA
BBA

www.bba-direct.com

Differential thermal effects on the energy distribution between photosystem II and photosystem I in thylakoid membranes of a psychrophilic and a mesophilic alga

Rachael Morgan-Kiss [a], Alexander G. Ivanov [b], John Williams [c], Mobashsher Khan [c], Norman P.A. Huner [b,*]

[a] *Department of Microbiology, University of Illinois, Urbana, IL 61801, USA*
[b] *Department of Plant Sciences, University of Western Ontario, London, ON, Canada N6A 5B7*
[c] *Department of Botany, University of Toronto, Toronto, ON, Canada*

Received 18 September 2001; received in revised form 19 December 2001; accepted 10 January 2002

Abstract

Sensitivity of the photosynthetic thylakoid membranes to thermal stress was investigated in the psychrophilic Antarctic alga *Chlamydomonas subcaudata*. *C. subcaudata* thylakoids exhibited an elevated heat sensitivity as indicated by a temperature-induced rise in F_o fluorescence in comparison with the mesophilic species, *Chlamydomonas reinhardtii*. This was accompanied by a loss of structural stability of the photosystem (PS) II core complex and functional changes at the level of PSI in *C. reinhardtii*, but not in *C. subcaudata*. Lastly, *C. subcaudata* exhibited an increase in unsaturated fatty acid content of membrane lipids in combination with unique fatty acid species. The relationship between lipid unsaturation and the functioning of the photosynthetic apparatus under elevated temperatures is discussed.

Keywords: Chloroplast membrane; Chlorophyll fluorescence; Heat stress; Lipid unsaturation; Photochemical apparatus; *Chlamydomonas subcaudata*

1. Introduction

The inhibitory effects of moderate to high temperatures in plants have been well documented [1], and the photosynthetic process is one of the most thermosensitive functions in the plant. While some of the causes underlying thermosensitivity in photosynthetic organisms still remain unclear, it has been well documented in plants [2,3] and algae [4,5] that the phenomenon of high temperature-induced sensitivity at the level of the thylakoid chlorophyll–protein complexes can be monitored indirectly via changes in specific chlorophyll fluorescence parameters. In particular, temperature-induced structural modulations

Abbreviations: ΔA_{820}, change in absorbance at 820 nm; ΔH, activation energy; Chl, chlorophyll; CPa, photosystem II core complex; CP1, photosystem I core complex; P_{700}, photosystem I reaction center; DBMIB, 2,5-dibromo-3-, methyl-6-isopropyl-*p*-benzoquinone; DGDG, digalactosyldiacylglycerol; $F_{688,699,700,715,722}$, 77 K fluorescence emission maxima at the respective wavelengths; FAME, fatty acid methyl ester(s); F_o, Chl *a* fluorescence of open reaction centers; F_q, maximal fluorescence yield in the absence of cations; FR, far red light; I_U, index of unsaturation; LHC, light harvesting complex; MGDG, monogalactosyldiacylglycerol; PG, phosphatidylglycerol; PS, photosystem; SQDG, sulfoquinovosyldiacylglycerol; *R*, distance between PSII and PSI chlorophyll–protein complexes; T_{CRIT}, critical temperature for maximum chlorophyll fluorescence

* Corresponding author. Fax: 519-661-3935.
E-mail address: nhuner@julian.uwo.ca (N.P.A. Huner).

0005-2736/02/$ – see front matter
PII: S0005-2736(02)00352-8

are manifested as a rise in minimal fluorescence (F_o) [1]. This fluorescence rise can be resolved into two major components. The first component is a gradual increase in fluorescence levels up to a threshold temperature. This threshold temperature is defined as the index of thermal stability of the photosynthetic membrane and has been used to classify species according to their tolerance to elevated temperatures [2]. The gradual rise in fluorescence is followed by a rapid increase in F_o up to a critical temperature, above which irreparable damage occurs to the membrane-bound photosynthetic complexes [6].

Several studies have shown that photosystem (PS) II appears to be one of the most thermosensitive pigment protein complexes [7,8]. The heat-induced increase in F_o fluorescence involves at least two major processes associated with functional/structural changes at the level of PSII. It has been well established that exposure to elevated temperatures causes reversible conversion of the major light harvesting antenna (light harvesting complex (LHC) II) from its trimeric to a monomeric form [7] followed by the physical dissociation of LHCII from the PSII core complex [8]. Beside that, the rise in F_o fluorescence has also been correlated with functional changes at the level of the PSII core. The accumulation of reduced Q_A in the dark [9,10] as well as an increase in the rate constant of $P680^+Pheo^-$ recombination [11] have been proposed as contributing events to the F_o rise. Lastly, the oxygen evolving complex is also heat labile [1] and thus the dissociation of the OEC from PSII may play some role in the heat-induced rise in fluorescence yields due to the build up of $P680^+$ centers [12].

In contrast to PSII, several studies have shown that PSI-mediated electron transport is stimulated at high temperatures [1,8,7,13,14]. This enhancement of PSI activity has been correlated with heat-induced leakiness of the thylakoid membranes to protons in conjunction with the uncoupling of linear electron transport [15], as well as destabilization of grana stacks [8,7]. This would allow exposure to additional stromal donors [16–18], which may enhance PSI-mediated cyclic electron transport. Lastly, heat-induced changes in the membrane organization have also been correlated with adjustments in the energy distribution between PSI and PSII [14,19,20], concomitant with changes in PSI and PSII absorptive cross-sections [14,21,22].

The contribution of the unsaturation of membrane lipids to enhance the tolerance of the photosynthetic machinery towards chilling stress has been well established and reviewed [23,24]. Plants [8,25] and algae [5,26] grown at low temperatures typically have higher levels of unsaturation of acyl chains in the membrane lipids. Conversely, plants grown at higher growth temperatures exhibit reduced levels of unsaturated fatty acids [25]. The adjustment in the lipid composition of the thylakoid membranes has been correlated with changes in the threshold temperature of F_o fluorescence [5], as well as the thermal stability of the chloroplast thylakoids [2]. In a recent paper, Murakami and co-workers [27] showed that transgenic tobacco lacking the ability to express the chloroplast trienoic fatty acid synthetase gene exhibited significantly higher rates of photosynthetic activity at elevated temperatures as well as the ability to survive higher growth temperatures than wild-type tobacco plants. This report is one of the first to provide a direct link between the proportion of unsaturated lipids found in the chloroplast photosynthetic membranes and the ability of the photosynthetic machinery to function at elevated temperatures [28].

The Antarctic alga *Chlamydomonas subcaudata*, one of the typical chlorophyte species found in Antarctic dry valley lakes [29], was isolated from the perennially ice-covered Lake Bonney, where the mean annual temperature is between −2 and 0°C [30]. We have previously established that *C. subcaudata* can only grow at temperatures lower than 18°C, and is classified as psychrophilic [31]. *C. subcaudata* grows optimally at around 8°C, in contrast with *Chlamydomonas reinhardtii*, a typical mesophilic species, which grows optimally at around 29°C [31]. Given the marked difference in thermal environments to which these two *Chlamydomonas* species are adapted, we investigated the thermal stability of the photosynthetic membranes and the membrane-bound pigment–protein complexes. In addition, we report the first compositional analysis of the membrane lipids and fatty acyl species in this Antarctic, psychrophilic, chlorophyte.

2. Materials and methods

2.1. Growth of algal cultures

Axenic isolates of *C. reinhardtii* (UTEX 89) and the Antarctic *C. subcaudata* [30] were grown as previously described in [31]. Cultures were grown under a low irradiance of 20 μmol photons m^{-2} s^{-1} that was similar to the natural irradiance environment of *C. subcaudata* [30] and were maintained in thermoregulated aquaria under optimal growth temperatures of either 29°C (*C. reinhardtii*) or 8°C (*C. subcaudata*). Total chlorophyll (Chl) content was determined according to [32].

2.2. Room temperature (F_o) Chl fluorescence

Fresh samples from mid-log cultures were incubated under a range of elevated temperatures for 5 min in the dark. Following the treatment, Chl fluorescence of whole cells was measured in vivo at the growth temperature (29 or 8°C) using a PAM-101 chlorophyll fluorescence detection system (Heinz Walz, Effeltrich, Germany). Chl fluorescence of open reaction centers (F_o) was obtained by excitation with a modulated measuring beam ($\lambda = 650$ nm, 0.12 μmol m^{-2} s^{-1}). The F_o signal was monitored using an Omnigraphic 2000 chart recorder (Bauch and Lomb). The critical temperature (T_{CRIT}) was determined at maximum F_o yields.

2.3. Low temperature (77 K) Chl fluorescence

Low temperature (77 K) Chl fluorescence emission of whole cells was excited at 436 nm and measured using a PTI LS-100 luminescence spectrophotometer (Photon Technology International, South Brunswick, NJ, USA) equipped with a liquid nitrogen device as described in [31]. All spectra represent an average of at least three independent experiments with three scans within each experiment. Samples from exponentially growing cultures were exposed to temperatures ranging from 15 to 65°C in the dark. Chlorophyll concentration ranged from 4 to 5 μg ml^{-1}. At various time intervals during the dark incubation, samples were quickly frozen in liquid nitrogen and 77 K fluorescence emission spectra were collected. The relative heat-induced changes in fluorescence emission at either 689 nm (ΔF_{689}) or 722 nm (ΔF_{722}), representing fluorescence associated with LCHII and PSI, respectively, were calculated as a percentage of controls and plotted as a function of time. Pseudo-first order rate constants (k) were estimated, and the activation energy (ΔH) was calculated as follows [33]:

$$\ln k = -\Delta H/RT + \Delta S/R \quad (1)$$

where k is first order rate constant, ΔH the activation energy (enthalpy), R the gas constant, T the temperature and ΔS the entropy.

The 77 K Chl fluorescence of samples treated at either the control (growth) temperatures or at T_{CRIT} were further analyzed via decomposition of the emission spectra. Decomposition analysis of the fluorescence emission spectra in terms of five Gaussian bands was carried out by a non-linear least squares algorithm that minimizes the chi-square function using a Microcal Origin Version 6.0 software package (Microcal Software, Northampton, MA, USA). The fitting parameters for the five Gaussian components, that is, position, area and full width at the half-maximum (FWHM), were free-running parameters.

2.4. Mg^{2+}-induced Chl fluorescence

The cation-induced increase in room temperature Chl fluorescence was measured following the procedure of Rubin et al. [34] as described earlier [35]. The fluorescence emission was measured using a PAM-101 chlorophyll fluorescence detection system. The reaction medium contained 10 mM Tricine-NaOH buffer (pH 8.0), 330 mM sucrose, 50 μM EDTA, 10 mM KCl. The samples were dark adapted and equilibrated for 2 min at the corresponding growth temperature of 8°C and 29°C for *C. subcaudata* and *C. reinhardtii*, respectively. After maximal fluorescence in the absence of cations was established, a final concentration of 10 mM $MgCl_2$ was added to the sample. The chlorophyll fluorescence increase was normalized to the maximal fluorescence yield for each sample. The mathematical analysis of the kinetics of the cation-induced fluorescence rise and the distance between PSII and PSI chlorophyll–protein complexes (R) was performed as in [36] using the following expression:

$$F/F_q - 1 = (R_o/R)^6 \quad (2)$$

where F and F_q are the maximum fluorescence yield of PSII in the presence and the absence of cations, respectively, and $R_o = 5$ nm is the average distance between the photosystems [37], assuming that the probability of exciton transfer from PSII to PSI is 50% [38].

2.5. Non-denaturing PAGE

Freshly isolated thylakoids (see [31]) at a Chl concentration of 50 μg ml^{-1} were incubated in the dark over a range of elevated temperatures (35–55°C) for 5 min. Chl–protein complexes were separated using a non-denaturing gel system as previously described [31]. Lanes were loaded on an equal Chl basis of 15 μg per lane. The excised lanes were scanned at 671 nm on a Beckman DU 640 spectrophotometer for Chl absorbance. The relative Chl content of each band was expressed as the peak area normalized to the total area of each scan.

2.6. Light-induced oxidation of P_{700}

Samples from cultures in mid-log phase were incubated at either the growth temperature or at the critical temperature (T_{CRIT}) in the dark for 5 min. The redox state of P_{700} was determined in vivo under ambient CO_2 conditions using a PAM-101 modulated fluorometer equipped with an ED-800T emitter-detector and PAM-102 units following the procedure of Schreiber at al. [39] essentially as described recently in [40].

2.7. Lipid extraction and analysis

Lipids were extracted from cells of *C. reinhardtii* and *C. subcaudata* according to Williams and Merrilees [41]. Fifty milliliters of fresh culture were centrifuged at 7000×*g* for 10 min and the pellet was resuspended in about 10 ml of a chloroform:methanol (2:1, v/v) solution and incubated on ice for 30 min. The samples were filtered through a column of pure cotton. Sephadex (G-25) was added to the resulting supernatant. The sample was then filtered twice and evaporated to dryness at 60°C under vacuum.

Lipids were separated by thin-layer chromatography and *trans*-esterified with 0.2 N HCl in dry methanol as previously described [42]. The fatty acid methyl esters (FAME) were analyzed by gas–liquid chromatography using a Hewlett-Packard model 5890 gas–liquid chromatograph (Hewlett-Packard, Mississauga, ON, Canada) with a 30 m×0.25 mm ID DB-225 capillary column (J&W Scientific, Folsom, CA, USA) programmed from 150 to 210°C at 3°C min^{-1}. FAME were estimated quantitatively from a methylpentadecanoate internal standard. Fatty acids were identified from known fatty acids in samples of *Brassica napus* and *Borago officinalis*. Other fatty acids were identified from retention times and comparison with the data from *C. reinhardtii* [43]. The unsaturation index (I_U) was calculated by multiplying the percentage of each fatty acid by the number of double bonds, and summing these results for all fatty acids identified in each sample.

3. Results

3.1. Effects of elevated temperatures on F_o levels

In agreement with earlier reports [1,14,20], both *C. reinhardtii* and *C. subcaudata* exhibited a typical rise in F_o fluorescences in response to incubation at elevated temperatures. The temperature at maximum F_o fluorescence (T_{CRIT}) observed in *C. reinhardtii* (50°C) is 10°C higher than that in *C. subcaudata* (40°C) (Fig. 1). However, *C. subcaudata* exhibited higher F_o levels than *C. reinhardtii* at incubation temperatures between 8°C and 45°C.

3.2. Heat-induced effects on low temperature fluorescence emission

Control *C. reinhardtii* cells exhibited typical 77 K fluorescence emission spectra with characteristic maxima at 688 nm, 699 nm and 717–722 nm associated with LHCII, PSII, and PSI core complexes, respectively (Fig. 2A) [31,44,45], while *C. subcaudata* exhibited much lower Chl fluorescence associated with PSI (Fig. 2C) [31,40]. Decomposition analysis of the 77 K fluorescence emission spectra yielded a best fit with five major spectral components in both samples (Fig. 2, Table 1) corresponding to the emis-

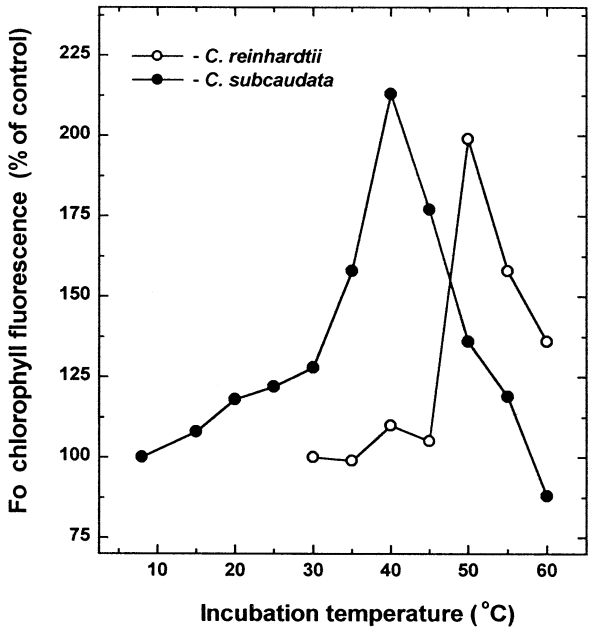

Fig. 1. Effect of exposure to elevated temperatures on minimal fluorescence (F_o) levels in whole cells of *C. subcaudata* (●) and *C. reinhardtii* (○). Samples were incubated in the dark under a range of elevated temperatures for 5 min. Values represent the percentage of control ($n = 3$).

sion subbands from light harvesting complex of PSII (680–685 nm), proximal antenna of PSII (688 nm), PSII core complex (697–700 nm) and PSI core complex (716–719 nm). The fifth spectral component (F_{vib}) centered around 740 nm corresponded to a number of small vibrational transitions in the near-infrared region [46,47]. Although the peak positions of all bands in control samples of both *Chlamydomonas* species were almost identical and within the expected range, the relative areas of subbands corresponding to PSI and PSII chlorophyll protein complexes differed significantly (Table 1). This resulted in a 10-fold higher area ratio of PSI- versus PSII-related bands in *C. reinhardtii* compared to *C. subcaudata*. Thus, the results of the spectral decomposition analysis revealed more dramatic differences in the PSII/PSI stoichiometry than the differences previously estimated simply on the basis of 77 K fluorescence emission peak intensities [31,40] (Table 1).

When whole cells of *C. reinhardtii* were heat treated at T_{CRIT}, a 2.5-fold increase in PSI-associated band area at 717 nm concomitant with a 2.5-fold decrease of the PSII-related band area at 699 nm

Table 1
Gaussian fitting parameters for the subband decompositions of 77 K chlorophyll fluorescence spectra of control and heat-treated (5 min) cells of *C. reinhardtii* and *C. subcaudata*

Parameters	*C. reinhardtii*		*C. subcaudata*	
	Control	Heat-treated	Control	Heat-treated
1 λ_{max}	684.8	679.4	684.4	683.9
FWHM	11.4	9.6	9.3	9.5
Area %	13.67	2.17	11.06	11.85
2 λ_{max}	688.7	687.9	688.1	687.9
FWHM	5.4	10.93	5.1	6.0
Area %	2.48	10.97	1.57	2.11
3 λ_{max}	697.2	699.8	697.9	698.6
FWHM	14.8	10.14	19.5	16.1
Area %	16.06	6.29	30.27	27.28
4 λ_{max}	717.2	716.8	718.9	716.1
FWHM	18.2	21.9	11.4	16.3
Area %	18.24	45.25	3.25	11.66
5 λ_{max}	732.3	739.0	738.5	734.6
FWHM	50.2	38.3	59.2	54.7
Area %	49.54	35.30	53.84	47.17
χ^2	0.00007	0.00011	0.00009	0.00016

The percentage areas of the spectral forms have been calculated from the total area given by the sum of all bands reported. The FWHM of each band is the sum of the left and right HWHM values. FWHM, full width at half-maximum; HWHM, half-width at half-maximum.

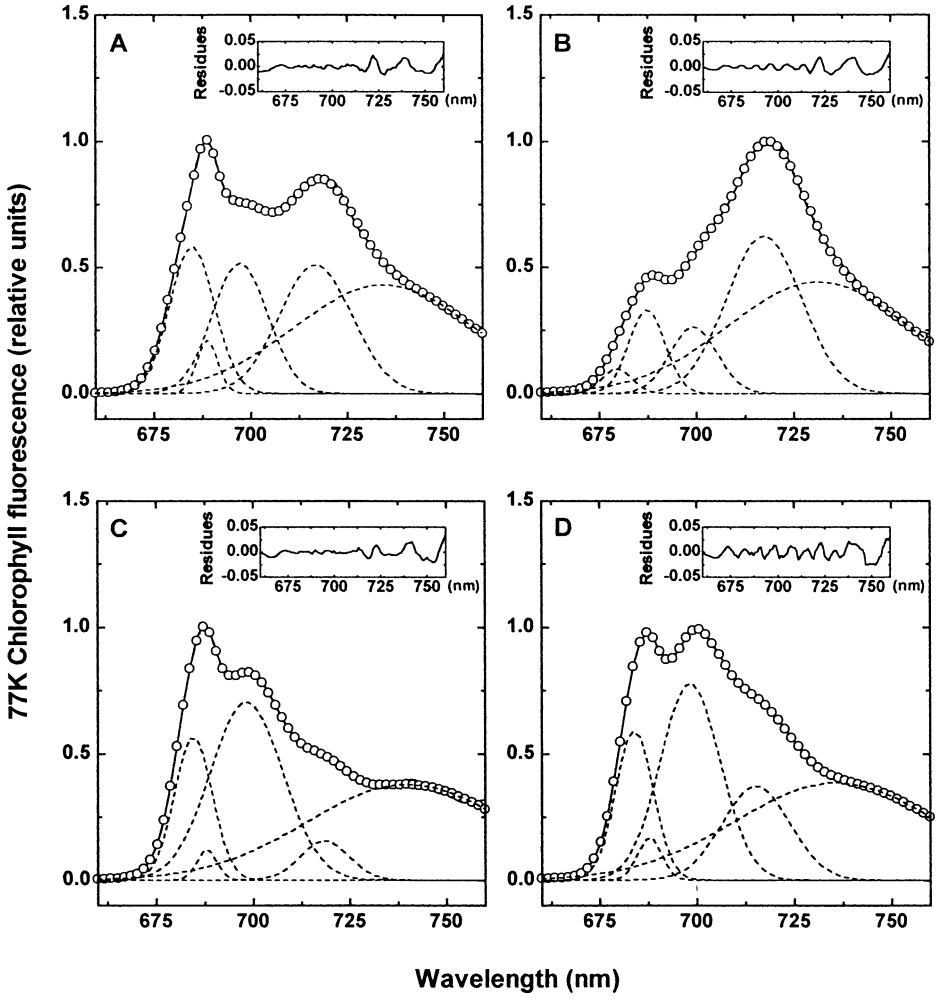

Fig. 2. Low temperature (77 K) chlorophyll fluorescence emission spectra and decomposition in Gaussian subbands of control (A,B,E,F) and heat-treated (C,D,G,H) *C. reinhardtii* (A–D) and *C. subcaudata* (E–H) whole cells. Chlorophyll fluorescence was excited at 436 nm. Cells from exponentially growing cultures were incubated in the dark for 5 min under growth temperatures of either 29°C (*C. reinhardtii*) or 8°C (*C. subcaudata*), or incubated for 5 min at T_{CRIT} of either 50°C (*C. reinhardtii*) or 40°C (*C.subcaudata*) before being quickly frozen in liquid nitrogen. Experimental curves represent averages of three scans in three independent measurements. ———, experimental curve; ○, sum of Gaussian subbands; - - -, Gaussian subband.

was observed (Fig. 2B; Table 1). These data indicate significant heat-induced redistribution of the excitation light energy in favor of PSI [14,19,20,47]. In addition, the band assigned to LHCII exhibited a blue shift from 685 to 679 nm, and its corresponding area was markedly reduced in heat-treated *C. reinhardtii* cells. Lastly, heat-treated samples of *C. reinhardtii* exhibited a 2-fold increase in the peak area of the band centered at 688 nm (Table 1).

In contrast, heat treatment of *C. subcaudata* did not induce any significant changes in the spectral characteristics of the LHCII-related bands at 685 and 688 nm. A modest decrease of 10% in the PSII-related band area accompanied by narrower band width was observed (Table 1). The most significant effects of heat treatment in the psychrophilic alga were registered in the PSI-associated peak, where there was a shift in the peak position from 719 to 716 nm, the band width of this spectral component was significantly increased and a 3.6-fold increase in the peak area was observed (Fig. 2D; Table 1). However, despite the apparent heat-induced effect

Table 2
Effects of heating on the stability of the Chl–protein complexes

Condition	CP1		CPa		$LHCII^1$:$LHCII^3$		FP
	Area	% of control	Area	% of control	Ratio	% of control	Area
C. reinhardtii							
Control	17.49	100	8.98	100	0.82	100	9.16
Heat-treated	17.45	100	4.96	55	0.43	52	9.24
C. subcaudata							
Control	15.17	100	15.65	100	1.41	100	4.66
Heat-treated	14.75	97	15.77	100	0.96	68	7.78

Thylakoids of *C. reinhardtii* and *C. subcaudata* were heated in the dark at the critical temperatures of 50°C and 40°C, respectively, and the Chl–protein complexes were separated via non-denaturing PAGE. Chl content was expressed as relative peak area as a function of the total area. CPa, photosystem II core; CP1, photosystem I core; $LHCII^1$, oligomeric light harvesting complex II; $LHCII^3$, monomeric LHCII ($n=2$); FP, free pigment.

on the PSI peak area, the PSI/PSII ratio in heat-stressed cells of *C. subcaudata* remained much lower (0.43) in comparison with the PSI/PSII ratio observed in *C. reinhardtii* (7.2) (Table 1).

Since the heat treatment appeared to have a pronounced differential effect on the fluorescence emission spectra of the two *Chlamydomonas* species (Fig. 2; Table 1) the activation energies for PSI and LHCII fluorescence maxima were determined. The activation energies for the increase in PSI fluorescence (ΔH_{722}) were identical for *C. reinhardtii* (99 ± 13 kJ) and *C. subcaudata* (100 ± 24 kJ). However, the activation energy associated with the increase in LHCII fluorescence (ΔH_{689}) of *C. subcaudata* (65 ± 18 kJ) was significantly lower than that of *C. reinhardtii* (114 ± 16).

3.3. Structural stability of chlorophyll–protein complexes

Non-denaturing electrophoretic separation of the thylakoid pigment–protein complexes from *C. reinhardtii* and *C. subcaudata* yielded several bands (data not shown) that were previously characterized in [31]. The presence of relatively low free pigment (less than 10% total Chl) indicated that the pigments remained associated with the protein complexes during heat treatment and subsequent solubilization and separation (Table 2).

In response to incubation over a range of elevated temperatures, the stability of PSII core complex, CPa, and oligomeric LHCII appeared to be similar for *C. subcaudata* and *C. reinhardtii* (Fig. 3B,C). However, at the level of PSI core complexes, CP1, *C. reinhardtii* appeared to exhibit greater stability to heat treatment than *C. subcaudata* (Fig. 3A).

When thylakoids were exposed to T_{CRIT}, CPa was less stable to heat treatment than CP1 in *C. reinhardtii*. In contrast, exposure to T_{CRIT} had no effect on the stability of CPa and minimal effects at the level of CP1 in *C. subcaudata* (Table 2). Furthermore, the ratio of oligomeric:monomeric LHCII in *C. reinhardtii* exhibited a 48% reduction, whereas *C. subcaudata* exhibited only a 32% decrease in $LHCII^1$:$LHCII^3$ in response to incubation at T_{CRIT} (Table 2).

Table 3
P_{700} parameters for whole cells of *C. reinhardtii* and *C. subcaudata* under control conditions versus heated treated at the critical temperatures of 50°C and 40°C, respectively

Condition	$\Delta A_{820}/A_{820}$ (P^+_{700})		$t^{red}_{1/2}$ (P^+_{700}) (ms)	
	Control	Heat treated	Control	Heat treated
C. reinhardtii	1.16 ± 0.1	1.82 ± 0.10	518 ± 24	1028 ± 133
C. subcaudata	0.78 ± 0.04	0.84 ± 0.06	342 ± 10	438 ± 65

$\Delta A_{820}/A_{820}$, change in absorbance at 820 nm; $t^{red}_{1/2}$ (P^+_{700}), half-time for re-reduction of P^+_{700}. Values represent means ± S.D. ($n=4$).

3.4. Effect of heat treatment on the redox state of P_{700}

Typical P_{700} transients presented in Fig. 4A,C and the data summarized in Table 3 indicate that the relative amount of far-red (FR) oxidized P_{700}^{+} ($\Delta A_{820}/A_{820}$) was 33% lower in *C. subcaudata* than in *C. reinhardtii* cells measured under control conditions. The kinetics of dark re-reduction of P_{700}^{+} after turning off the FR light, representing mainly the extent of cyclic electron flow around PSI [40], was 1.5-fold faster in *C. subcaudata* versus *C. reinhardtii* under control conditions (Table 3). Furthermore, under control conditions, both algal species exhibited a fast re-reduction of P_{700}^{+} to a steady state redox level of the P_{700} pool; however, this transient was less apparent in *C. subcaudata* than in *C. reinhardtii* (Fig. 4A,C). As discussed in [40], this transient is an indication of electron flow to the PQ pool via external stromal donor(s).

In response to incubation at T_{CRIT}, *C. reinhardtii*

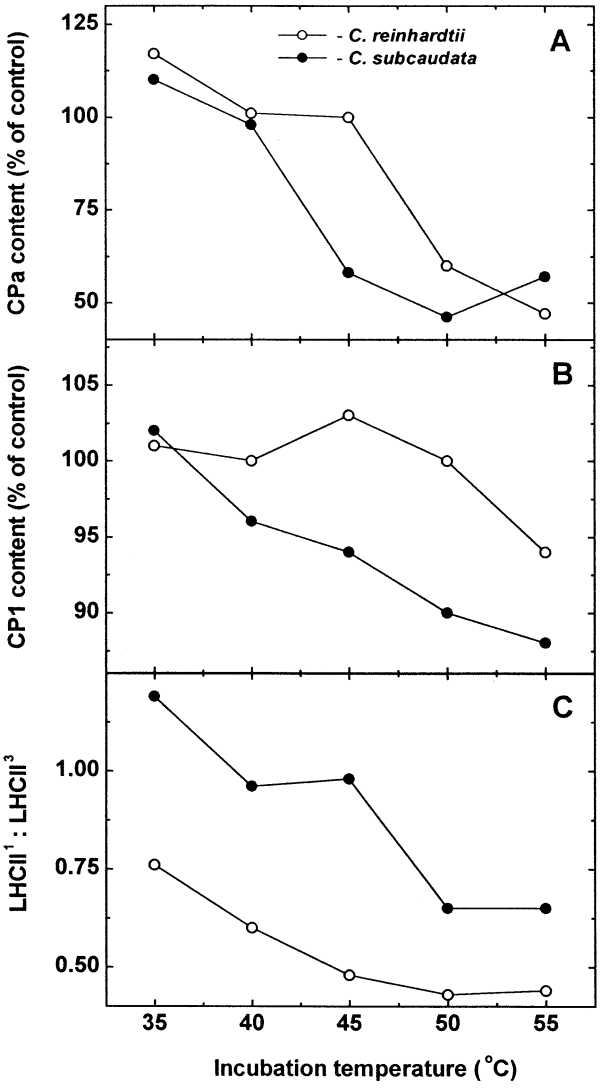

Fig. 3. Effect of heat treatment on the stability of the Chl–protein complexes. Freshly isolated thylakoids of *C. reinhardtii* (○) and *C. subcaudata* (●) were incubated for 5 min in the dark under a range of elevated temperatures. Relative amounts were estimated as the Chl content of the Chl–protein bands from a non-denaturing PAGE. (A,B) Changes in CP1 (PSI core) (A) and CPa (PSII core) (B) content were expressed as percentages of control non-heated samples. (C) Changes in $LHCII^{1}$:$LHCII^{3}$ (oligomeric:monomeric LHCI) were expressed as the absolute ratio ($n=2$).

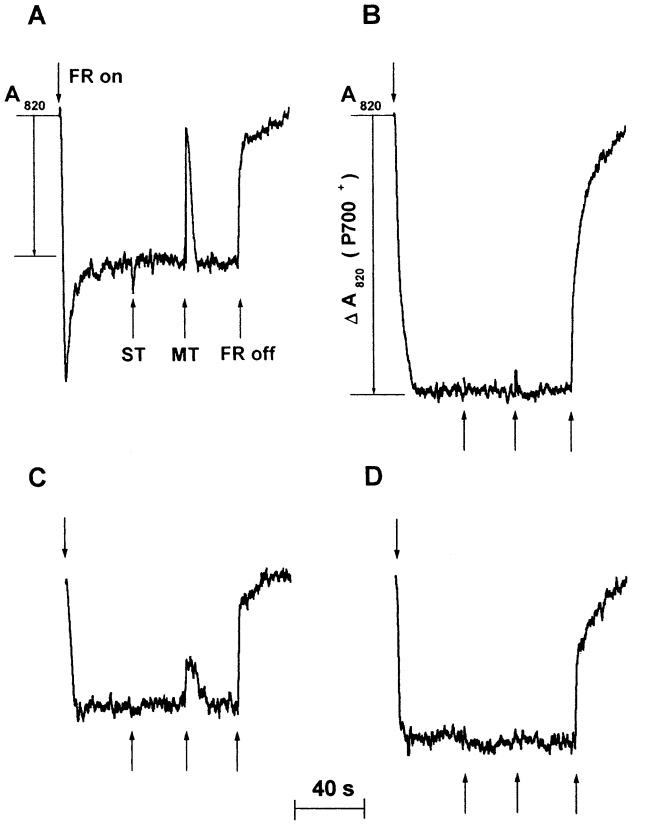

Fig. 4. In vivo measurement of the redox state of P_{700} in control and heat-treated cells of *C. reinhardtii* (A,B) and *C. subcaudata* (C,D). (A,C) Whole cells were incubated in the dark for 5 min under the growth temperature. (B,D) Samples were incubated for 5 min in the dark at T_{CRIT} of 50°C in *C. reinhardtii* (B) and 40°C in *C. subcaudata* (D). The steady state oxidation of P_{700} ($\Delta A_{820}/A_{820}$) was estimated after the far red light was turned on (FR on) and the half-time for the re-reduction of P_{700}^{+} was estimated after the far red light was turned off (FR off). MT, multiple-turnover flash; ST, single-turnover flash.

responded by increasing the extent of the P_{700}^{+} signal by 36% (Fig. 4A,B; Table 3). Exposure of *C. reinhardtii* to T_{CRIT} also inhibited the initial transient re-reduction of P_{700}^{+} (Fig. 4A,B). In contrast, there was no significant change in the extent of P_{700}^{+} signal in heated samples of *C. subcaudata* (Fig. 4C,D; Table 3). Lastly, heat treatment induced a doubling in the rate of dark re-reduction of P_{700}^{+} in *C. reinhardtii*, while *C. subcaudata* exhibited only about a 20% increase in the half-time of P_{700}^{+} dark re-reduction (Table 3).

3.5. Cation-induced increase of chlorophyll fluorescence

The typical kinetic curves of Mg^{2+}-induced fluorescence increase for cultures grown under control temperatures are presented in Fig. 5. As expected, after the establishment of the maximal fluorescence (F) in samples of fresh cultures resuspended in a low salt medium, the addition of $MgCl_2$ induced a rapid rise in the fluorescence yield in both *Chlamydomonas* species (Fig. 5). When compared at their respective growth temperatures, 8°C-measured samples of *C. subcaudata* exhibited a 1.4-fold higher initial fluorescence yield (F) and a 1.3-fold lower value for the Mg^{2+}-dependent fluorescence increase (ΔF) in comparison with 29°C *C. reinhardtii* (Fig. 5; Table 4). These trends were observed regardless of the measuring temperature (Table 4), indicating that differences in measuring temperature could not account for the differential response observed between the two *Chlamydomonas* species. *C. subcaudata* exhibited a 3.2-fold slower half-time for the fluorescence rise in comparison with *C. reinhardtii* when measured at the respective growth temperatures of 8 and 29°C. However, when both species were measured at 29°C, both *Chlamydomonas* species exhibited similar values for $t_{1/2}$ (Table 4).

It has been previously demonstrated that the spill-over-type excitation energy transfer from PSII to PSI [48,49] depends mainly on the distance (R) between the photosystems [36], and in the absence of Mg^{2+} approximately half of the PSII excitons are transferred to PSI [38]. Following the kinetic analysis proposed in [36], the traces of cation-induced increase of PSII fluorescence (Fig. 5) were converted to the kinetics of an increase of the distance (R) between both photosystems (Fig. 6). Assuming that the process occurs in a viscous medium, and combining the hypothesis of Förster-type energy transfer between the two photosystems, the analysis proposed in [36] shows that the slope of R versus time (Fig. 5) is directly proportional to the ratio between the frictional coefficient of the thylakoid membranes and the coulombic force which monitors the increase in distance between the chlorophyll–protein complexes of PSII and PSI. Based on this analysis, *C. subcaudata* exhibited a lower slope than *C. reinhardtii*, which would indicate that the distance between PSII and PSI is larger in *C. subcaudata* in comparison with *C. reinhardtii*.

3.6. Lipid analysis

The total fatty acid content as well as the fatty acid composition of the individual membrane lipids of *C. reinhardtii* (Tables 5 and 6) were very similar to

Table 4
Parameters of Mg^{2+}-induced chlorophyll fluorescence rise in cell suspensions of *C. reinhardtii* and *C. subcaudata* measured at the corresponding growth temperatures of 29°C and 8°C, respectively

Sample	F	ΔF	$\Delta F/\Delta F+F$	$t_{1/2}$ (s)
C. reinhardtii				
M29/20 at 29°C	67.82 ± 3.21	50.96 ± 4.13	0.427 ± 0.028	4.19 ± 0.10
M29/20 at 8°C	68.80 ± 1.34	70.28 ± 0.29	0.505 ± 0.005	31.47 ± 2.44
C. subcaudata				
P8/20 at 8°C	93.30 ± 2.55	38.97 ± 1.98	0.294 ± 0.013	13.47 ± 1.98
P8/20 at 29°C	87.69 ± 1.58	35.32 ± 0.54	0.287 ± 0.002	4.98 ± 0.07

F, initial fluorescence level observed before addition of $MgCl_2$; ΔF, maximum fluorescence change observed after addition of 10 mM $MgCl_2$; $t_{1/2}$, time for chlorophyll fluorescence increase to $\Delta F/2$. Mean values ± S.E. were calculated from 3–6 independent measurements.

those reported in [42]. By contrast with *C. reinhardtii*, *C. subcaudata* exhibited an 18:2 species of unknown identity as well as 18:4(6,9,12,15), but lacked 18:3(5,9,12) and 18:4(5,9,12,15) (Table 5). In general, *C. subcaudata* exhibited higher levels of unsaturation than *C. reinhardtii* (Table 5). The unsaturation index (I_U) for *C. subcaudata* was estimated as 2.74 in comparison with an I_U of 1.90 in *C. reinhardtii*.

In monogalactosyldiacylglycerol (MGDG), the major fatty acid species in *C. subcaudata* were 16:4, 18:3, and 18:4, while the major species in *C. reinhardtii* were 16:4, 18:3, and 18:1. In addition, *C. reinhardtii* exhibited small amounts of the less unsaturated 16 and 18C fatty acids, which were not detected in *C. subcaudata* (Table 6). Ratios of C_{16}/C_{18} were similar between the two species (Table 6).

The fatty acid composition and C_{16}/C_{18} ratios of digalactosyldiacylglycerol (DGDG) exhibited similar trends as were observed for MGDG (Table 6). The

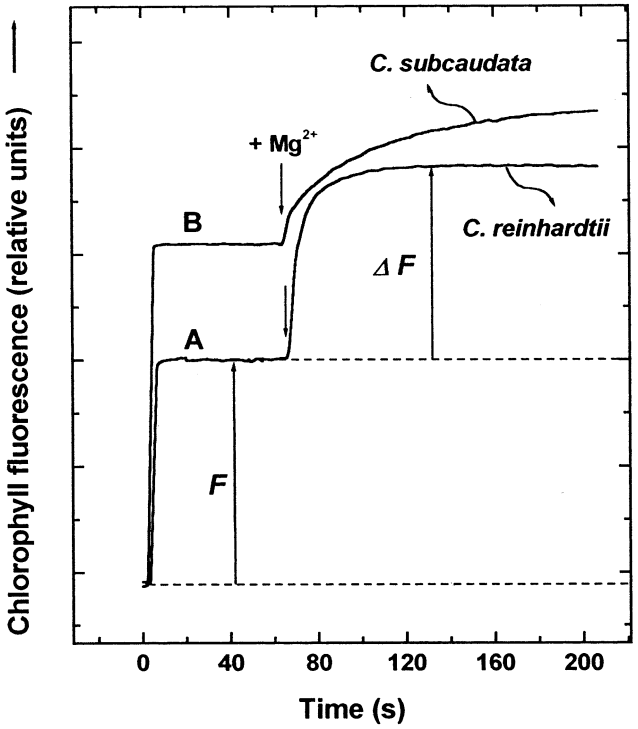

Fig. 5. Typical kinetic traces of Mg^{2+}-induced chlorophyll fluorescence increase in *C. reinhardtii* (A) and *C. subcaudata* (B) cell suspensions. The arrows indicate the addition of 10 mM $MgCl_2$. *F*, fluorescence intensity before addition of Mg^{2+}; ΔF, maximal fluorescence registered after Mg^{2+} addition. All other experimental conditions are given in Section 2.

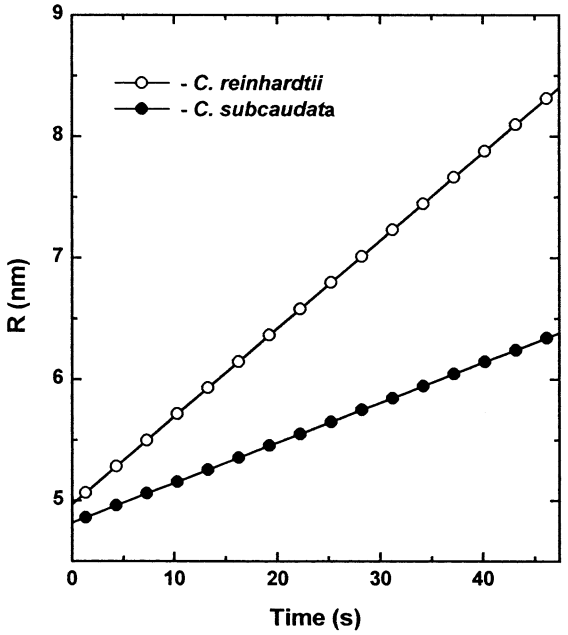

Fig. 6. Kinetics of the rate of salt-induced increase in the distance *R* between PSII and PSI chlorophyll–protein complexes upon addition of 10 mM $MgCl_2$ in *C. reinhardtii* (○) and *C. subcaudata* (●) cell suspensions. The *R* values were estimated from the kinetic analysis of the curves similar to those presented in Fig. 5, using expression 2, as described in [36]. Mean values ± S.E. were calculated from three independent experiments.

Table 5
Fatty acid composition (mol%) of the total lipid extracted from *C. reinhardtii* and *C. subcaudata* cells grown at 20 μmol m^{-2} s^{-1} and either 29 or 8°C, respectively

Fatty acid	*C. reinhardtii*	*C. subcaudata*
14:0	ND	1.4 ± 1.2
16:0	18.7 ± 0.5	9.5 ± 0.9
16:1(7)	5.1 ± 0.4	Tr
16:1(*trans*-3)	2.8 ± 0.2	1.7 ± 0.1
16:2(7,10)	Tr	Tr
16:3(7,10,13)	2.4 ± 0.0	1.9 ± 0.2
16:4(4,7,10,13)	13.9 ± 0.1	25.6 ± 0.8
18:0	4.7 ± 0.7	Tr
18:1(9)	15.5 ± 1.0	6.1 ± 0.4
18:1(11)	15.5 ± 1.0	3.7 ± 1.0
18:2(?)	Tr	2.4 ± 0.2
18:2(9,12)	3.2 ± 0.3	2.0 ± 0.2
18:3(5,9,12)	5.1 ± 0.4	ND
18:3(9,12,15)	21.5 ± 0.3	36.0 ± 1.0
18:4(5,9,12,15)	3.7 ± 0.7	ND
18:4(6,9,12,15)	Tr	8.5 ± 0.4

The exact identity of 18:2(?) is not known. Tr, trace (< 1%); ND, not detected. Values represent means ± S.D. ($n = 3$).

major fatty acid species in DGDG of *C. subcaudata* were 16:0, 16:4 and 18:3 with low levels of 18:1. In contrast, in *C. reinhardtii* the major fatty acid species of DGDG were 16:0, 18:1 and 18:3, with no detectable levels of 16:4 (Table 6).

The two *Chlamydomonas* species differed significantly in the fatty acid composition of sulfoquinovosyldiacylglycerol (SQDG). As previously reported [43], *C. reinhardtii* exhibited high levels of 16:0 and lower amounts of 18:0, 18:1 species, and 18:3(9,12,15) (Table 6). In marked contrast, the major fatty acid content associated with SQDG from *C. subcaudata* was 16:0, 16:4 and 18:3. Thus, the C_{16}/C_{18} ratio of SQDG was comparable with MGDG and DGDG in *C. subcaudata*, while the C_{16}/C_{18} ratio of SQDG was about 2-fold higher in *C. reinhardtii* (Table 6).

In phosphatidylglycerol (PG), the levels of 16:0 and 16:1 (*trans*-$^3\Delta$) were higher in *C. reinhardtii* than in *C. subcaudata*, while *C. subcaudata* exhibited significant levels of 14:0 (Table 6). The trend in higher levels of unsaturated 18C fatty acids in *C. subcaudata* was also observed at the level of PG, in particular the levels of 18:3 (Table 6). However, the ratio of C_{16}/C_{18} was similar between the two species (Table 6).

Table 6
Fatty acid composition of the major membrane lipids of *C. reinhardtii* and *C. subcaudata* grown at 29°C/20 μmol m^{-2} s^{-1} and 8°C/20 μmol m^{-2} s^{-1}, respectively

Fatty acid	Diacylglycerol (mol%)			
	MGDG	DGDG	SQDG	PG
C. reinhardtii				
14:0	ND	Tr	ND	Tr
16:0	2.0 ± 0.6	32.3 ± 0.7	86.4 ± 2.3	31.6 ± 1.0
16:1*	8.0 ± 0.5	11.0 ± 0.4	Tr	33.9 ± 2.6
16:2(7,10)	1.0 ± 0.0	Tr	ND	Tr
16:3(7,10,13)	4.0 ± 0.4	3.3 ± 0.0	ND	ND
16:4(4,7,10,13)	27.8 ± 3.3	ND	ND	Tr
18:0	Tr	1.1 ± 0.2	1.5 ± 0.1	2.6 ± 0.3
18:1(9)	16.5 ± 2.8	25.9 ± 0.6	3.3 ± 0.5	14.2 ± 0.3
18:1(11)	1.7 ± 0.8	4.9 ± 0.4	3.7 ± 0.6	5.0 ± 0.6
18:2(9,12)	1.7 ± 0.2	3.2 ± 0.1	ND	4.5 ± 0.2
18:3(5,9,12)	Tr	2.0 ± 0.4	ND	ND
18:3(9,12,15)	33.0 ± 0.9	14.3 ± 0.3	4.0 ± 0.4	5.8 ± 0.7
18:4(5,9,12,15)	2.4 ± 0.5	1.4 ± 0.2	ND	Tr
C_{16}/C_{18}	43	47	87	67
C. subcaudata				
14:0	Tr	1.7 ± 1.7	Tr	10.5 ± 0.3
16:0	Tr	10.6 ± 1.4	32.9 ± 2.1	16.6 ± 1.0
16:1*	Tr	Tr	Tr	24.7 ± 1.2
16:2(7,10)	Tr	Tr	Tr	2.1 ± 1.8
16:3(7,10,13)	1.0 ± 0.1	6.1 ± 1.5	1.3 ± 0.2	Tr
16:4(4,7,10,13)	45.0 ± 0.2	23.3 ± 2.5	9.3 ± 1.6	6.6 ± 1.5
18:0	Tr	Tr	Tr	Tr
18:1(9)	Tr	3.5 ± 0.5	2.6 ± 0.2	1.8 ± 0.5
18:1(11)	Tr	2.5 ± 0.7	6.6 ± 0.8	5.8 ± 1.4
18:2(?)	Tr	Tr	Tr	Tr
18:2(9,12)	1.1	2.6 ± 0.2	2.4 ± 0.2	2.0 ± 0.2
18:3(9,12,15)	35.3 ± 0.5	44.5 ± 2.2	38.5 ± 1.1	24.4 ± 0.2
18:4(6,9,12,15)	15.8 ± 0.5	3.6 ± 0.3	4.0 ± 0.5	4.6 ± 1.2
C_{16}/C_{18}	47	43	44	61

*16:1(*trans*-^{3}) in PG; 16:1(*cis*-^{7}) in the other lipids.
Tr, trace (< 1%); ND, not detected.
Values represent means ± S.D. ($n = 3$).

4. Discussion

In conjunction with numerous earlier reports in plants and algae [6,8,14], exposure of either *C. subcaudata* or *C. reinhardtii* to short-term heat stress resulted in a typical heat-induced increase of the room temperature F_o fluorescence up to a critical temperature; however, *C. subcaudata* exhibited a T_{CRIT} that was 10°C lower than that of *C. reinhardtii* (Fig. 1). This is in agreement with previous reports that lower threshold temperatures for the heat-induced rise in F_o fluorescence have been observed in low temperature-grown plants and algae in comparison with those acclimated to moderate temperatures [5,25]. In addition, Raison et al. [25] observed that an increase in lipid fluidity in low temperature-grown plants correlated with lower threshold temperatures for the thermal stability of the thylakoid membranes. While our study did not directly measure membrane fluidity, higher membrane fluidity has been linked with higher unsaturation of the acyl chains [48] and could explain the lower T_{CRIT} in the psychrophilic alga since a considerably higher unsaturation index was estimated in *C. subcaudata* in comparison with *C. reinhardtii* (Table 5).

Several possible functional and/or structural changes in the photosynthetic apparatus have been proposed to contribute to the heat-induced rise in F_o fluorescence. The increase in F_o levels has been attributed to the dissociation of LHCII [7,8,38] from the PSII core as well as inhibition of the PSII-dependent photochemical activity via heat-induced damage to the donor site [9–12]. In support of these findings, the heat-induced blue shift in the 77 K fluorescence emission peak corresponding to the LHCII complex from 685 nm to 679 nm in *C. reinhardtii* (Table 1) could be indicative of disassociated light harvesting complexes [49,50] in the mesophilic alga. Furthermore, the rise in the F_o fluorescence might be also due, in part, to a selective degradation and loss of function at the level of the PSII core (CPa), as indicated by the loss in structural stability of CPa in heat-treated *C. reinhardtii* cells (Table 2). Inhibition of electron transport from Q_A to Q_B [52,53] as well as dark reduction of Q_A [54] via the chloroplast Ndh complex reduction of the plastoquinone pool [55] have been also suggested as potential causes for the heat-induced rise in F_o. Thus, the activation of a substantial dark stromal electron flow that was previously reported in *C. reinhardtii* [40] may be enhanced under elevated temperatures and could have contributed to the heat-induced rise in F_o.

In contrast with *C. reinhardtii*, heat-treated *C. subcaudata* cells at a T_{CRIT} of 40°C exhibited neither a significant shift of the LHCII peak (Table 1) nor thermal instability at the structural level of CPa (Table 2). Furthermore, we have previously suggested that there is minimal contribution from stromal reductants to the dark reduction of the plastoquinone pool in *C. subcaudata* [40]. Hence, it appears that the cause of the rise in F_o fluorescence in *C. subcaudata* is distinct from the postulated heat-induced functional and/or structural adjustments in the photosynthetic apparatus of *C. reinhardtii* as described above. One possible explanation to account for the rise in F_o in the psychrophilic alga could be a higher degree of heat-induced aggregation of LHCII into supramolecular arrays in heat-treated cells of *C. subcaudata* [56]. In support of this suggestion, heat-stressed thylakoids of *C. subcaudata* exhibited a higher ratio of oligomeric to monomeric LHCII (0.96) as compared to *C. reinhardtii* (0.42) (Table 2), which could be an indication of the formation of LHCII aggregates.

While a state II to state I transition has been correlated with the heat-induced rise in F_o fluorescence [3], we believe that our results agree with previous reports that heat treatment in *C. reinhardtii* (Fig. 2A,B) mimics a state I to II transition [14,19,20,47]. In support of this, the 77 K ratio of relative fluorescence emitted from PSI (717–719 nm) to that of PSII (697–700 nm) shifted from 1.13 in control cells to 7.19 in heat-stressed *C. reinhardtii* cells (Table 1), indicating an adjustment of the excitation energy distribution between the photosystems [45]. Furthermore, a redistribution of light energy that favors PSI fluorescence emission should be accompanied by a concomitant decrease in LHCII fluorescence yields. In *C. reinhardtii*, the activation energy for the decrease in PSII fluorescence was similar to the activation energy for the increase in PSI fluorescence.

In contrast with the significant heat-induced redistribution of the excitation energy in favor to PSI in *C. reinhardtii*, heat-stressed *C. subcaudata* exhibited only a modest decrease in PSII fluorescence (10%) and a smaller increase of the PSI/PSII fluorescence ratio (Fig. 2C,D; Table 1). However, it should be

mentioned that even the initial PSI/PSII fluorescence ratio in control non-heat-treated *C. subcaudata* was also markedly lower (0.11) than in control *C. reinhardtii* cells (1.13). Thus, we believe that the lower PSI/PSII fluorescence ratio in heat-treated *C. subcaudata* might not reflect only the lower capacity for heat-induced energy redistribution, but could be also associated with altered composition and/or stoichiometry of the major components of the photosynthetic apparatus. Indeed, in previous papers we have demonstrated that the abundance of PsaA/PsaB polypeptides of the PSI reaction center is drastically reduced and the PSI/PSII ratio is much lower in *C. subcaudata* (0.71) as compared to *C. reinhardtii* (1.43) [31], as well as the absence of state transitions in the psychrophilic alga [40]. Most probably, these differences reflect the adaptation response of *C. subcaudata* to its natural environment of extremely low light and predominantly PSII exciting blue–green spectral range [30].

Consistent with previous reports demonstrating heat-induced increase of PSI-related photochemical activities [1,7,8,47], *C. reinhardtii* cells exposed to heat stress exhibited the expected stimulation of P_{700} photoxidation (Fig. 4, Table 3). Additionally, the heat-induced increase in P_{700} photoxidation in *C. reinhardtii* was most pronounced at a comparable temperature (T_{CRIT}) to the heat-induced rise in F_o as well as the increase in the 77 K fluorescence ratio of PSI/PSII (data not shown). Thus, although the precise mechanism(s) for this phenomenon is still unclear [57], it appears likely that spillover-type changes in the energy distribution probably contributed, in part, to the stimulation of photoxidation of P_{700} in heat-treated cells of *C. reinhardtii*. This is in agreement with earlier studies indicating that alteration of the excitation energy distribution in favor of PSI results in an increased yield of P_{700} photoxidation by about 25% [58,59]. Furthermore, Ivanov and Velitchkova [47] attributed the heat-induced stimulation of P_{700} photoxidation to an increase in the relative PSI absorptive cross-section. While the absorptive cross-sections were not measured in our experiments, it is well documented that adjustments of 77 K fluorescence emission correlate well with changes in the functional absorptive cross-sections of PSI and PSII [47,60]. This response could indicate a short-term mechanism to protect against photoxidative damage of PSI under conditions which preferentially inhibit PSII-mediated electron transport [16]. More recently, it has been demonstrated that exposure of *C. reinhardtii* to heat stress significantly enhanced (chloro)-respiratory electron transport, which in turn suppressed the activity of the linear photosynthetic electron transport activity at the level of the cytochrome b_6/f complex [61]. This would result in the prevention of the reduction of P_{700}^{+} from electron flow through the cytochrome b_6/f complex and would resemble the effect of 2,5-dibromo-3-, methyl-6-isopropyl-*p*-benzoquinone (DBMIB) on P_{700} photoxidation. In support of this hypothesis, recent findings indicated that DBMIB poisoning of *C. reinhardtii* cells induced a similar stimulatory effect on P_{700} photoxidation [40] as was observed in heat-treated cells (Fig. 4).

In contrast with *C. reinhardtii*, exposure of *C. subcaudata* to T_{CRIT} did not result in any significant effects on the P_{700} photoxidation (Fig. 4, Table 3). Reynolds and Huner [17] observed in rye that plants grown under non-cold hardening conditions exhibited a heat-induced stimulation of PSI-mediated electron transport, while cold-hardened plants did not exhibit a heat-induced effect at the level of PSI activity. These authors argued that the cold-hardened plants showed maximal PSI activities under control conditions, and thus were unable to exhibit a further stimulation of PSI in response to heat stress [17]. Thus, it could be suggested that cells of *C. subcaudata*, which possess relatively low levels of PSI [31] and relatively high rates of cyclic electron transport [40], also exhibit maximal levels of P_{700} oxidation under control conditions and are therefore unaffected at the level of PSI by incubation at elevated temperatures.

Further data concerning the spillover type of redistribution of light energy were derived from Mg^{2+}-induced increase of chlorophyll fluorescence. It is generally assumed that the salt-induced increase of chlorophyll fluorescence is associated with the lateral segregation of chlorophyll–protein complexes of PSII and PSI and reflects the decrease in excitation energy transfer 'spillover' from PSII to PSI [49]. Since *C. subcaudata* and *C. reinhardtii* exhibited comparable maximal fluorescence yields after addition of Mg^{2+} (ΔF), it appears that an efficient cation-dependent energy redistribution exists in both *Chlamydomonas*

species. In fact, *C. subcaudata* exhibited a 1.5-fold lower value in comparison with *C. reinhardtii* for the relative change in Chl fluorescence (Table 4), which would indicate a higher capacity for spill-over-type energy between the photosystems in the psychrophilic versus the mesophilic alga. This difference between the two *Chlamydomonas* species could not be accounted for by differences in the measuring temperature (Table 4). In contrast, the half-time for the Mg-induced rise in Chl fluorescence was sensitive to the measuring temperature, which agrees with previous observations that the salt-induced rise in Chl fluorescence and the concomitant lateral segregation of the photosystems are diffusion-controlled processes [34,49]. However, while the half-times were comparable between the 29°C-measured samples of *C. reinhardtii* and *C. subcaudata*, at 8°C *C. reinhardtii* exhibited a 2.5-fold lower rate of Chl fluorescence rise in comparison with *C. subcaudata* (Table 4). We believe that this latter observation indicates differences within the thylakoid dynamic properties between the two *Chlamydomonas* species.

It seems plausible that the overall higher levels of unsaturated acyl chains observed in *C. subcaudata* (Table 5) could indicate higher fluidity of the membrane lipids in *C. subcaudata* in comparison to *C. reinhardtii*. Furthermore, *C. subcaudata* exhibited the unique fatty acids species, 14:0, 18:4(6,9,12,15) and an unknown 18:2 fatty acid, that were not detected in *C. reinhardtii*, but lacked 16:1(7), 18:0, 18:3(5,9,12) and 18:4(5,9,12,15) (Table 5). In addition, *C. subcaudata* exhibited differences in the fatty acid composition of specific lipid classes in comparison with *C. reinhardtii*, most notably SQDG (Table 6). Both the presence of the unique fatty acids and the differences in the fatty acid composition associated with SQDG would also affect the fluidity of the membranes [2]. Lastly, it has recently been shown that the level of polyunsaturated fatty acids, specifically the trienoic fatty acid content of the thylakoid membranes, directly affects photosynthetic rates and the ability of the plant to survive elevated temperatures [27]. In support of this work, recent experiments in our laboratory indicate that photosynthesis rates are inhibited at lower temperatures in *C. subcaudata* versus *C. reinhardtii* (T. Pocock, N. Huner, unpublished data). Thus, the presence of higher levels of polyunsaturated fatty acids observed in the psychrophilic alga may play a key role in the elevated thermosensitivity of the photosynthetic process of the Antarctic alga.

In conclusion, the increased heat sensitivity at the level of the photosynthetic thylakoid membranes, indicated by the temperature-induced increase in F_o fluorescence, observed in *C. subcaudata* was a consequence of an increase in unsaturated fatty acid of the membranes lipids in combination with unique fatty acid species in the psychrophilic alga. However, this apparent thermal sensitivity of the photosynthetic membranes was not accompanied by changes at either the structural level of PSII or the functional level of PSI in *C. subcaudata*. The absence of a heat-induced effect at the level of P_{700} photoxidation in the Antarctic alga may reflect either the lack of external stromal donors or the lower capacity to redistribute light energy in favor of PSI. Lastly, the stimulation of PSI observed in *C. reinhardtii* might reflect a short-term mechanism to protect against PSI photo-destruction during environmental stresses that selectively inhibit PSII-mediated electron transport [16]. The absence of this acclimatory strategy in *C. subcaudata* probably reflects a loss of such short-term acclimatory mechanisms as a result of adaptation to extremely stable, low growth temperatures.

5. For further reading

[51]

Acknowledgements

The authors are indebted to Dr. J. Priscu for his generous gift of an axenic culture of *C. subcaudata*. We thank Mr. Ian Craig of the Faculty of Science, Photographic, Imaging and Consulting Service at the University of Western Ontario for his assistance. This work was supported by the Natural Science and Engineering Research Council of Canada.

References

[1] J. Berry, O. Bjorkman, Annu. Rev. Plant Physiol. 31 (1980) 491–543.

[2] M. Havaux, H. Greppin, R.J. Stasser, Planta 186 (1991) 88–98.
[3] J. Ravenel, G. Peltier, M. Havaux, Planta 193 (1994) 251–259.
[4] N.A. Gaevskii, G.A. Sorokina, V.M. Gol'd, V.G. Ladygin, A.V. Gekhman, Fiziol. Restenii 32 (1986) 674–680.
[5] D.V. Lynch, G.A. Thompson, Plant Physiol. 74 (1984) 198–203.
[6] U. Schreiber, J. Berry, Planta 136 (1977) 233–238.
[7] T.S. Takeuchi, J.P. Thornber, Aust. J. Plant Physiol. 21 (1994) 759–770.
[8] P.A. Armond, O. Björkman, L.A. Staehelin, Biochim. Biophys. Acta 601 (1980) 433–442.
[9] J. Cao, Govindjee, Biochim. Biophys. Acta 1015 (1990) 180–188.
[10] V. Goltsev, I. Yordanov, T. Tsonev, Photosynthetica 30 (1994) 629–643.
[11] J.-M. Briantais, J. Dacosta, Y. Goulas, J.-M. Ducret, I. Moya, Photosynth. Res. 48 (1996) 189–196.
[12] T. Yamashita, W.L. Butler, Plant Physiol. 43 (1968) 2037–2040.
[13] K. Gounaris, A.P.R. Brian, P.J. Quinn, W.P. Williams, FEBS Lett. 153 (1983) 47–52.
[14] A.G. Ivanov, M.I. Kitcheva, A.M. Christov, L.P. Popova, Plant Physiol. 98 (1992) 1228–1232.
[15] M.A. Stidham, E.G. Uribe, G.J. Williams, Plant Physiol. 69 (1982) 163–165.
[16] M. Havaux, Photosynth. Res. 47 (1996) 85–97.
[17] T.L. Reynolds, N.P.A. Huner, Plant Physiol. 93 (1990) 319–324.
[18] P.G. Thomas, P.J. Quinn, W.P. Williams, Planta 167 (1986) 133–139.
[19] P.V. Sane, T.S. Desai, V.G. Tatake, Govindjee, Photosynthetica 18 (1984) 439–444.
[20] E. Weis, Plant Physiol. 74 (1984) 402–407.
[21] A.V. Ruban, V.V. Trach, Photosynth. Res. 29 (1991) 157–169.
[22] C. Sundby, A. Melis, P. Mäenpää, B. Andersson, Biochim. Biophys. Acta 851 (1986) 475–483.
[23] H. Wada, Z. Gombos, N. Murata, Proc. Natl. Acad. Sci. USA 91 (1994) 4273–4277.
[24] I. Nishida, N. Murata, Annu. Rev. Plant Physiol. Plant Mol. Biol. 47 (1996) 541–568.
[25] J.K. Raison, J.K.M. Roberts, J.A. Berry, Biochim. Biophys. Acta 688 (1982) 218–228.
[26] D.V. Lynch, G.A. Thompson, Plant Physiol. 74 (1984) 193–197.
[27] Y. Murakami, M. Tsuyama, Y. Kobayashi, H. Kodama, K. Iba, Science 287 (2000) 476–479.
[28] T.D. Sharkey, Science 287 (2000) 435–437.
[29] D.M. McKnight, B.L. Howes, C.D. Taylor, D.D. Goehringer, J. Phycol. 36 (2000) 852–861.
[30] P.J. Neale, J.C. Priscu, Plant Cell Physiol. 36 (1995) 253–263.
[31] R.M. Morgan, A.G. Ivanov, J.C. Priscu, D.P. Maxwell, N.P.A. Huner, Photosynth. Res. 56 (1998) 303–314.
[32] S.W. Jeffrey, G.F. Humphrey, Biochem. Physiol. Pflanz. 167 (1975) 191–194.
[33] K.E. van Holde, Plant Physiol. 74 (1985) 402–407.
[34] B.T. Rubin, J. Barber, G. Paillotin, W.S. Chow, Y. Yamamoto, Biochim. Biophys. Acta 851 (1981) 475–483.
[35] M.Y. Velitchkova, A.G. Ivanov, J. Plant Physiol. 142 (1993) 144–150.
[36] C. Vernotte, J.M. Briantias, B. Maison-Peteri, Biochim. Biophys. Acta 681 (1982) 11–14.
[37] F.A. Wollman, J. Olive, P. Bennoun, M. Recouvrier, J. Cell Biol. 87 (1980) 728–735.
[38] U. Schreiber, P.A. Armond, Biochim. Biophys. Acta 502 (1988) 138–151.
[39] A.G. Ivanov, R. Morgan, G.R. Gray, M.Y. Velitchkova, N.P.A. Huner, FEBS Lett. 430 (1998) 288–292.
[40] R.M. Morgan-Kiss, A.G. Ivanov, N.P.A. Huner, Planta 214 (2002) 435–445.
[41] J.P. Williams, P.A. Merrilees, Lipids 5 (1970) 367–370.
[42] M. Khan, J.P. Williams, Lipids 28 (1993) 953–955.
[43] C. Giroud, A. Gerber, W. Eichenberger, Plant Cell Physiol. 19 (1988) 587–595.
[44] J. Garnier, J. Maroc, D. Guyon, Biochim. Biophys. Acta 851 (1986) 395–406.
[45] S. Lin, R.S. Knox, Photosynth. Res. 27 (1991) 157–168.
[46] G.H. Krause, E. Weis, Annu. Rev. Plant Physiol. Plant Mol. Biol. 42 (1991) 313–349.
[47] A.G. Ivanov, M.Y. Velitchkova, J. Photochem. Photobiol. B Biol. 4 (1990) 307–320.
[48] J. Barber, FEBS Lett. 118 (1980) 1–10.
[49] J. Barber, Annu. Rev. Plant Physiol. 33 (1982) 261–295.
[50] A.W.D. Larkum, J. Anderson, Biochim. Biophys. Acta 679 (1982) 410–421.
[51] J.E. Mullet, C.J. Arntzen, Biochim. Biophys. Acta 589 (1980) 100–117.
[52] J.M. Ducruet, Y. Lemoine, Plant Cell Physiol. 26 (1985) 419–429.
[53] N.G. Bukhov, S.C. Sabat, P. Mohanty, Photosynth. Res. 23 (1990) 81–87.
[54] Y. Yamane, T. Shikanai, Y. Kashino, H. Koike, K. Satoh, Photosynth. Res. 63 (2000) 23–34.
[55] L.A. Sazanov, P.A. Burrows, P.J. Nixon, FEBS Lett. 429 (1998) 115–118.
[56] A.V. Ruban, P. Horton, Biochim. Biophys. Acta 1102 (1992) 30–38.
[57] N.G. Bukhov, P. Mohanty, in: G.S. Singhal, G. Renger, S.K. Sopory, K.-D. Irrgang, Govondjee (Eds.), Concepts in Photobiology: Photosynthesis and Photomorphogenesis, Kluwer Academic Publishers, Narosa Publishing House, 1999, pp. 617–648.
[58] J. Biggins, Biochim. Biophys. Acta 504 (1978) 288–297.
[59] A. Telfer, H. Bottin, J. Barber, P. Mathis, Biochim. Biophys. Acta 764 (1984) 324–330.
[60] J.H. Argyroudi-Akoyunoglou, C. Vakirtzi-Lemonias, Arch. Biochem. Biophys. 253 (1987) 38–47.
[61] F. Lajkó, A. Kadioglu, G. Borbély, G. Garab, Photosynthetica 33 (1997) 217–226.